RF-heating and plasma confinement studies in the HANBIT mirror device

2003 Nucl. Fusion 43 686

(http://iopscience.iop.org/0029-5515/43/8/308)

Nucl. Fusion 43 (2003) 686–691 PII: S0029-5515(03)65481-5

RF-heating and plasma confinement studies in the HANBIT mirror device

M. Kwon[1], J.G. Bak[1], K.K. Choh[1], J.H. Choi[1], J.J. Choi[2], J.W. Choi[1], K.S. Chung[2], Y.S. Chung[1], A.C. England[1], J.S. Hong[1], H.G. Jhang[1], B.C. Kim[1], J.Y. Kim[1], S.S. Kim[1], W.C. Kim[1], M.C. Kyum[1], W.H. Ko[1], B.J. Lee[1], D.K. Lee[1], H.G. Lee[1], S.G. Lee[1], T.H. Lho[1], H.K. Na[1], B.H. Park[1], D.C. Seo[1], S.H. Seo[1], H.R. Yang[1], S.J. Yoo[1], K.I. You[1] and N.S. Yoon[2]

[1] Korea Basic Science Institute, 52 Yeoeun-dong, Yusung-ku, Daejeon 305-333, Korea
[2] HANBIT User Group

E-mail: kwonm@kbsi.re.kr

Received 15 October 2002, accepted for publication 13 June 2003
Published 18 July 2003
Online at stacks.iop.org/NF/43/686

Abstract
HANBIT is a magnetic mirror confinement device. Recently, after finishing the first campaign for the basic system development, it started the second campaign for high-temperature plasma confinement physics study in a mirror configuration. Here, we introduce briefly the HANBIT device and report initial physics experiment results on RF-plasma heating and confinement in the simple mirror configuration. It appears that the discharge characteristics of HANBIT are quite different from those in other mirror devices, and an explanation is presented to clarify the difference.

PACS numbers: 52.55.jd, 52.50.Qt, 52.35.Mw, 52.80.Pi

1. Introduction

HANBIT is a magnetic mirror confinement device, refurbished from the old TARA machine [1]. After re-installation of the main vacuum-vessel system in Korea in 1995, the main effort had been in developing and improving basic heating and diagnostic systems over the first-phase from 1996 to 2000 [2]. Recently, with achievement of the first-phase goal, HANBIT started the second-phase campaign for high-temperature plasma physics study in a mirror configuration. Here, we introduce briefly the HANBIT mirror device and report initial physics experiment results of plasma production, heating, stability, and confinement in the HANBIT device.

As will be described in more detail later, the overall dimension and configuration of HANBIT are similar to the original TARA. HANBIT has, however, a difference in that the anchor and plug each exist only on one end, which is mainly due to the fact that it has been reconstructed utilizing the half-section of the original TARA. Even with this asymmetric configuration, it is basically possible to study the MHD stabilization by the anchor or the confinement improvement by thermal barrier formation in the plug (e.g. see the recent work [3–5]). During the initial physics experiments, however, we have concentrated more on the basic physics studies of RF-heating, stability, and confinement in the simple mirror configuration of the central-cell. The scheme based on the RF-ponderomotive or side-band coupling effect [6, 7] has been explored to provide the basic stabilization of the MHD interchange mode in this configuration. The other stabilization schemes using the anchor or a hot-electron ring, and the confinement improvement using the thermal barrier or RF-plugging are to be studied in the future. It is also noted that HANBIT has mainly used a 500 kW RF-power system with a slot antenna for plasma production and heating. As is well-known, the slot antenna was originally developed for the slow wave beach heating in TARA [3], but here we try to utilize it for plasma production and heating in the fast wave and ion cyclotron resonance heating (ICRH) regimes.

In section 2 we introduce briefly the overall magnetic configuration, RF-heating, and diagnostics systems in the HANBIT device. The initial physics results are then presented and discussed in section 3, and finally a conclusion and future work plan are given in section 4.

2. HANBIT mirror device

The HANBIT mirror device consists of a simple mirror-type central cell, an anchor, a plug, and two end tanks. The anchor with a minimum-B configuration and the plug of a simple mirror type are attached at each end of the central cell, and then connected to the fan and cusp tanks, respectively. The central cell has a length of about 5 m, a limiter radius of 0.18 m, a B-field intensity of 0.1–0.3 T (at the mid-plane), and a mirror ratio of about 10. Figure 1 shows the overall magnetic configuration and antenna locations in the HANBIT device.

For plasma production and heating, HANBIT mainly uses a 500 kW RF amplifier in the frequency range of 3.2–15 MHz with a slot antenna located near mid-plane of central cell. As shown in figure 2, the slot antenna has the configuration, which is basically a mixture of the well-known double-half turn (DHT) [8] and Nagoya-type-III antennae [9]. Thus, it can be used to excite the $m = \pm 1$ fast and/or slow waves through the DHT part or produce initial plasmas through the E_z field of Nagoya-type part. In addition to this 500 kW slot antenna system, HANBIT also has a 100 kW DHT antenna system near the mirror throat, which is to be utilized for the fast wave or beach heating in the near future. Besides these RF systems, HANBIT has a 2 kW, 14 GHz Klystron system in the plug for pre-ionization and hot-electron ring experiments. A 200 kW, 28 GHz gyro-klystron system is also under installation in central cell for ECH experiment.

For the measurement of plasma parameters, HANBIT also has many diagnostic tools, including a microwave interferometer, electrostatic probes, a Thomson scattering system, diamagnetic loops, a charge-exchange neutral particle analyser, H-alpha monitors, VUV/XUV spectrometers, an end-loss-ion energy analyser (ELA), etc. In addition, several new diagnostics, such as a reflectometer, diagnostic neutral beam system, x-ray crystal spectroscopy, soft x-ray imaging system, Fabry–Perot interferometer, and laser-induced florescence (LIF) system, are under test or development.

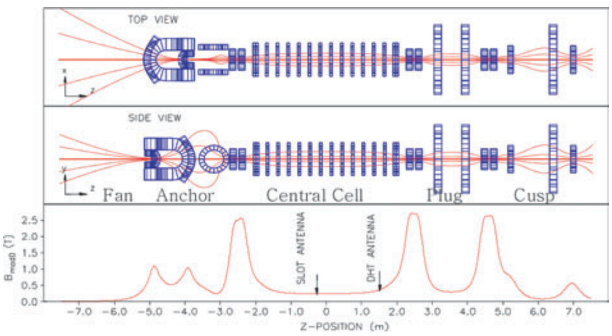

Figure 1. Overall magnetic configuration and antenna locations in HANBIT.

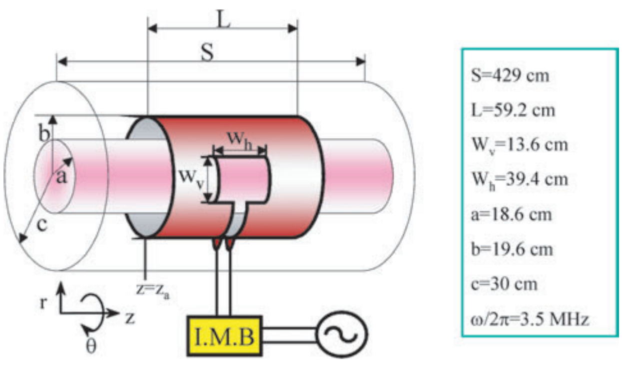

Figure 2. A schematic view of HANBIT slot antenna system.

3. Initial physics experimental results and discussion

Initial physics experiments have been mainly focused on identifying discharge characteristics and on getting stable plasma production and operational modes, utilizing the 500 kW slot-antenna system and varying discharge conditions such as fuelling rate, RF power, and B-field intensity in central cell (B_{cc}). RF-power waveform and matching condition have been also adjusted to get an optimum plasma production. It appears that the slot antenna system works well for the initial plasma production in various conditions when we supply a proper pre-filling gas pressure in the range of a few times 10^{-4} Torr. This relatively high neutral pressure is believed to be necessary since the breakdown occurs mainly by the E_z-field of slot antenna, to which the usual Townsend-type breakdown condition is applied. In figure 3, we show a typical RF-power waveform and line-integrated density evolution with a successful plasma production in HANBIT.

Unlike the initial plasma production, subsequent plasma heating and plasma parameter evolution appear to be sensitive to the discharge conditions. Particularly, discharge characteristics are found to have a significant difference between the two regimes of $\omega > \omega_{ci}$ and $\omega < \omega_{ci}$, suggesting the existence of two distinct operational modes, where ω is the RF frequency and ω_{ci} is the ion cyclotron frequency at the mid-plane of central cell. A typical example is shown in figure 4, where a big jump in plasma line-density and plasma beta is observed around $B_{cc} \sim 106\%$ (which corresponds to $B_{cc} \sim 0.23$ T where the ion cyclotron resonance condition, $\omega \sim \omega_{ci}$ is satisfied), when we vary B_{cc} over the range of 0.12–0.3 T (or $\omega/\omega_{ci} \sim 0.8$–1.9) at a fixed RF frequency of $\omega = 3.5$ MHz. Recent data show further that the density profile, ion temperature, and wall recycling rate, etc have also a substantial change at $\omega \sim \omega_{ci}$. For example, the plasma density profile is almost flat over most of plasma region in the $\omega > \omega_{ci}$ case, but changes to a radially peaked profile in the $\omega < \omega_{ci}$ case, as shown in figure 5. The plasma ion temperature measured by the end-loss analyser also shows a big increase by about 3–4 times when ω becomes smaller than ω_{ci} [10]. Furthermore, the wall-recycling rate appears to increase substantially in the $\omega < \omega_{ci}$ regime. As shown in figure 6, the neutral pressure increases during the discharge, even though there is no additional fuelling, in the 110% shot, while the discharge stops in the 104% shot. Note this increase in the wall recycling rate in the $\omega < \omega_{ci}$ regime is correlated well with the ion temperature increase and resulting fast neutrals generation through charge exchange process.

It is interesting to note here that these results in HANBIT are quite different from what has been observed in the other mirror devices, such as HIEI [9] and Phadrus or Phadrus-B [6, 8]. A main conclusion from these previous studies was that MHD stable, high-density plasma modes with a radially peaked density profile can be obtained well in the $\omega > \omega_{ci}$ regime. A possible explanation of this difference between HANBIT and the other devices may be now found if we note that, as pointed out by Majeski *et al* [8], in order to get a stable high-density plasma in the $\omega > \omega_{ci}$ regime it is critical to excite a radially peaked plasma wave, such as the $m = +1$ fast wave, which can then provide a stabilization of the MHD interchange instability through the ponderomotive force. In

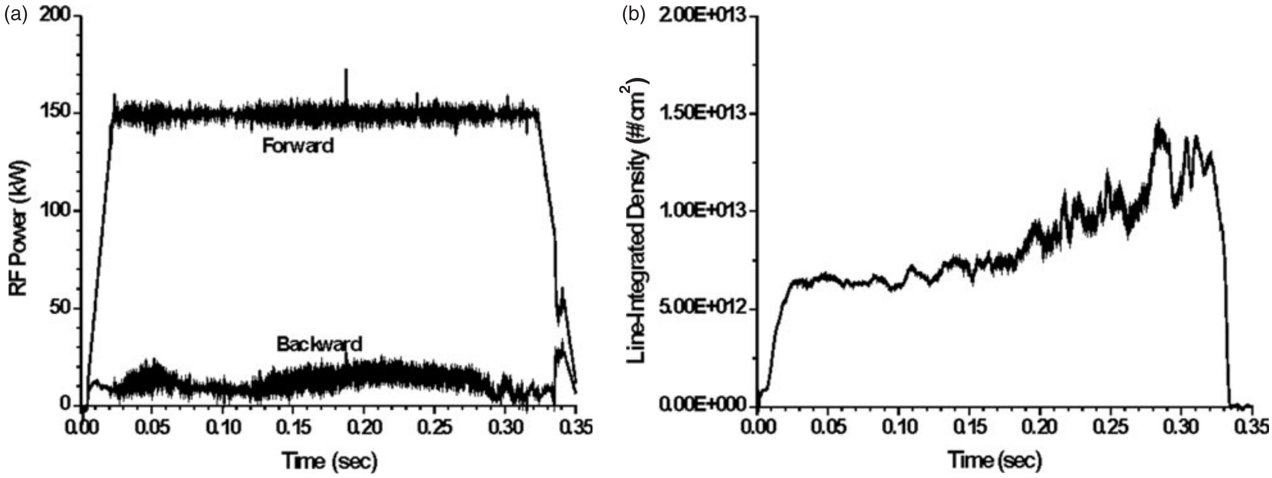

Figure 3. A typical RF-power waveform and line-density evolution.

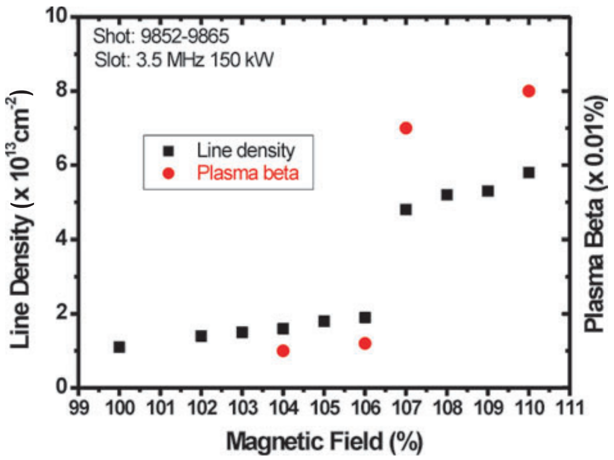

Figure 4. Variations of peak line-density and plasma beta as a function B_{cc}.

other words, this means that a well-designed antenna, which can excite the fast wave in the target plasma, is essential to get a stable high-density plasma mode in the $\omega > \omega_{ci}$ regime.

If we now compare the slot antenna in HANBIT with the DHT antenna in Phadrus-B [8], it is found that, while both can excite the $m = +1$ fast wave, the dominant parallel wavelength of the slot antenna is about four times shorter than that of the DHT antenna. This may be understood noting that the HANBIT slot antenna was originally developed for the excitation of the slow wave, of which the parallel wavelength is generally shorter than that of the fast wave. Reminding then that the parallel wavelength of a fast wave in a uniform plasma decreases with plasma density, like $\lambda_{||} \propto (n_e)^{-1/2}$ (this is particularly true when ω is near ω_{ci}), we can see that for a proper coupling with the fast wave the HANBIT slot antenna requires the target plasma density about one order larger than the DHT antenna in Phadrus-B. From the usual dispersion relation in the uniform cold plasma, it is indeed estimated that the optimum density for a good antenna–plasma coupling is of the order of 10^{12} cm^{-3} for the HANBIT slot antenna, while of the order of 10^{11} cm^{-3} for the Phadrus-B DHT antenna. We note that in Phadrus-B the initial plasma is produced by ECH, up to the order of $n_e \sim 10^{11}$ cm^{-3}. This meets well the optimum density condition for the fast wave excitation in Phadrus-B, providing an explanation of why stable high-density plasma modes can be produced well there. Meanwhile, in the HANBIT device the initial plasma is mainly produced from the E_z field of the slot antenna. Clearly, the plasma density obtainable by the E_z field heating will depend on the input RF-power, fuelling amount, confinement time, etc. It is not clear yet how much power or what condition is necessary to produce the target plasma density of the order of 10^{12} cm^{-3} for the HANBIT slot antenna. However, it can be shown that at a given input power condition the possibility to buildup such a high density is much larger in the $\omega \leqslant \omega_{ci}$ case, compared with the $\omega > \omega_{ci}$ case. This may then provide an explanation why the stable high-density modes are much easily obtained in the $\omega \leqslant \omega_{ci}$ case, than the $\omega > \omega_{ci}$ one, in HANBIT.

To see how a larger density build-up is possible in the $\omega \leqslant \omega_{ci}$ case, we first remember that a slow wave can exist, in addition to the fast wave, in the $\omega \leqslant \omega_{ci}$ regime. Since the parallel wavelength of the slow wave is usually shorter than the fast wave, it can now couple to the slot antenna even in the low-density regime of order 10^{11} cm^{-3}. This means that there is now a large possibility for the slow wave to be excited, during the plasma production period by the E_z field, in the $\omega < \omega_{ci}$ regime. When the slow wave is excited near $\omega \sim \omega_{ci}$, a strong ion heating is expected through the ion cyclotron resonance over a bandwidth of $\Delta\omega = |\omega_{ci} - \omega| < k_{||} V_{ti}$, where $k_{||}$ and V_{ti} are the parallel wave-number of the slow wave and the ion thermal velocity, respectively. We note the observed increase in the ion temperature and the wall-recycling rate in the $\omega < \omega_{ci}$ regime in HANBIT is well correlated with this slow-wave excitation model.

It is now shown that the ion heating by the slow wave can enhance greatly the density build-up even at the same power of E_z field. First, we note that in the simple mirror configuration the confinement time is almost determined by the parallel loss-cone transport. By the ambipolar diffusion condition the confinement time is then almost determined by the ion transport, increasing with the ion temperature. As shown in figure 7, a calculation of the parallel particle confinement time using the well-known Pastukhov formula [11] in HANBIT

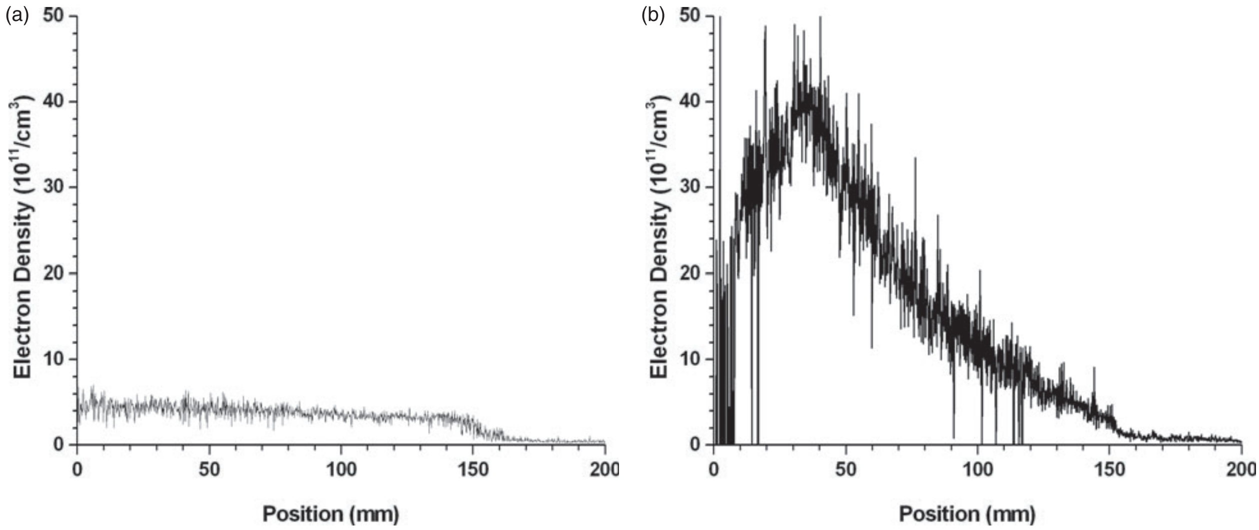

Figure 5. Plasma density profiles when (*a*) $B_{cc} \sim 104\%$ or $\omega/\omega_{ci} = 1.03$ and (*b*) $B_{cc} \sim 110\%$ or $\omega/\omega_{ci} = 0.97$ with the same RF input power of 150 kW.

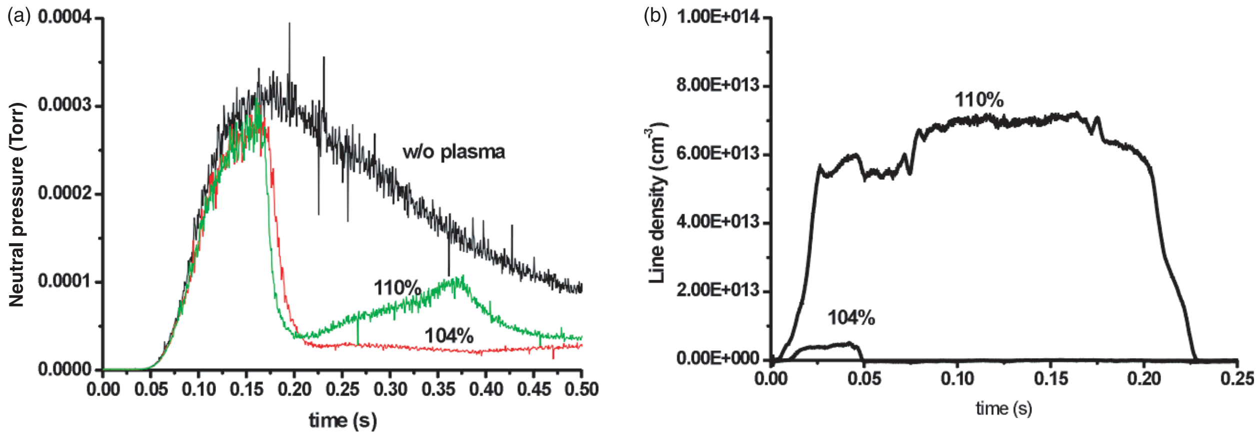

Figure 6. The evolutions of neutral pressure and line-integrated density for the two cases of 104%, and 110% when we give only an initial fuelling before the shot (also shown is the neutral pressure evolution of a dummy shot without plasma).

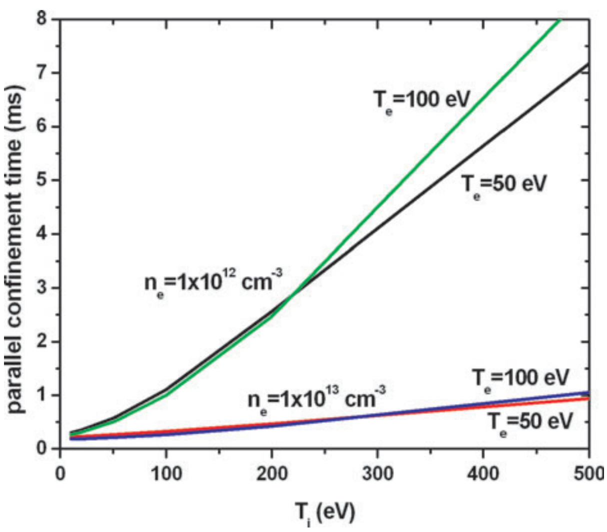

Figure 7. Ion temperature dependence of parallel particle confinement time in HANBIT model.

device model indicates that a substantial increase in the confinement time is indeed possible by increasing the ion temperature when the plasma density is relatively low. It is noted that this increase in the confinement time is well correlated with the behaviour of ambipolar potential, which also increases with the ion temperature. Second, we find that the MHD stability can be also improved by the excitation of the slow wave, supporting the build-up of larger density gradient near edge. To see this, we first show a typical structure of RF wave-field in figure 8, which was calculated using a RF code [12] in a simple cylinder model with an uniform plasma density and the HANBIT slot antenna model of figure 2.

Utilizing the following well-known formula of the RF-ponderomotive force [6, 13], we can see

$$F_{\mathrm{P}} = \frac{-e^2}{4m_{\mathrm{i}}}\left[\frac{\nabla_r E_+^2}{\omega_{\mathrm{ci}}(\omega-\omega_{\mathrm{ci}})} - \frac{\nabla_r E_-^2}{\omega_{\mathrm{ci}}(\omega+\omega_{\mathrm{ci}})} + \frac{m_{\mathrm{i}}}{m_{\mathrm{e}}}\frac{\nabla_r E_z^2}{\omega^2}\right]$$

First that the E_z field from the slot antenna gives stabilization near the edge since it has the near-field profile of $\partial|E_z|/\partial r > 0$ in the inside region of plasma boundary, as shown in figure 8.

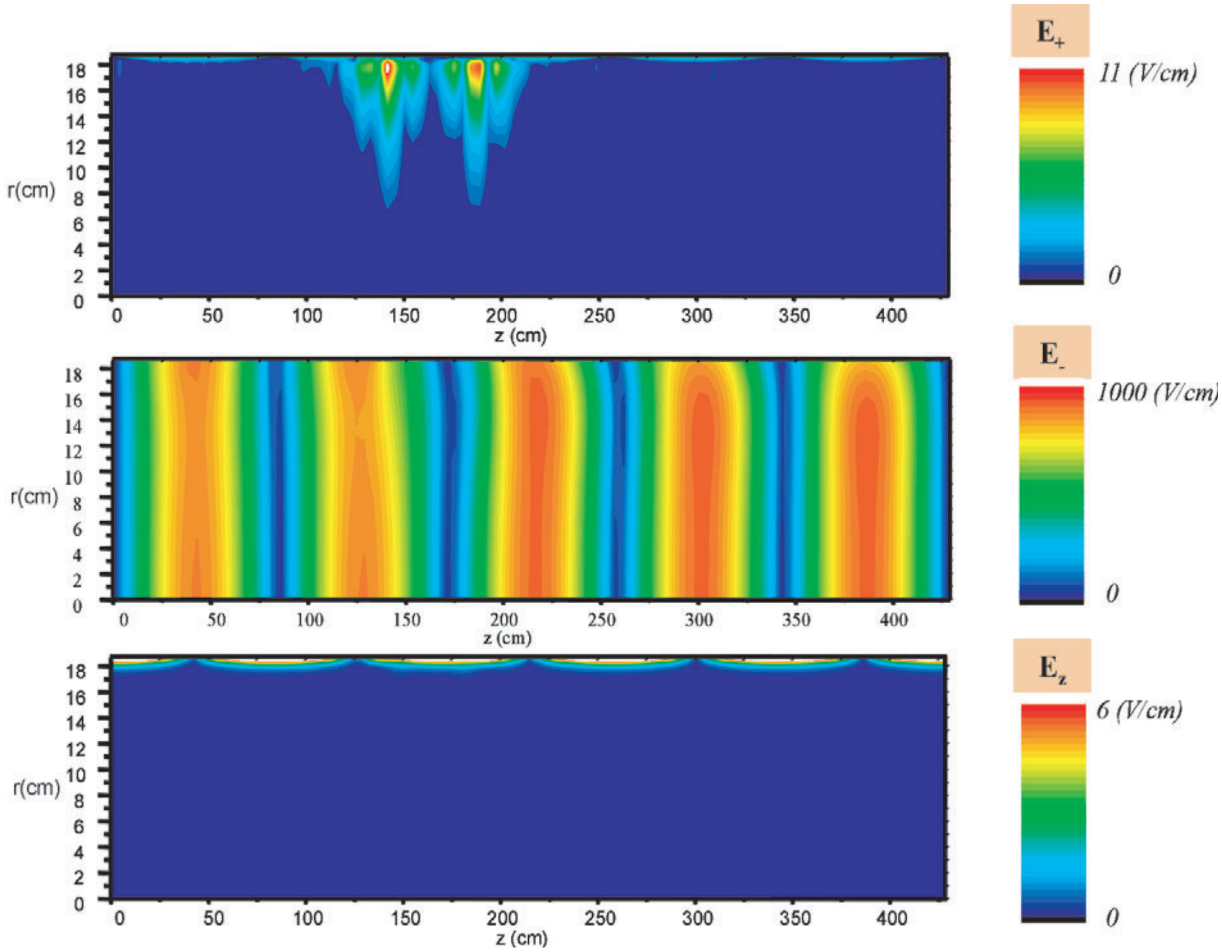

Figure 8. A typical RF wave-field structure calculated in the cylindrical plasma model with a uniform density of 1×10^{12} cm^{-3} and the HANBIT slot antenna in figure 2.

It is believed that this stabilizing effect from the E_z field may mainly support the small edge density build-up during the initial plasma production. Unlike the E_z field, the slow wave (which is typically left-hand polarized or has mainly the component of E_+) is more like a plasma wave being excited in the plasma region. It is, however, expected to be rapidly damped near the surface by the ICRH in HANBIT with no beach heating, so having the profile peaked near edge, but inside of the plasma boundary, as shown in figure 8. An additional stabilizing ponderomotive force is then possible from the slow wave in the outside region of the peak point, making a steeper density gradient build-up feasible near the edge. (In addition to this stabilization, the slow wave can also contribute to the destabilization at the inside region of the peak point, but here the stability will be dominated by the fast wave or the second term with E_- field in the above formula, which is indeed a main force to provide the stability for a radially peaked profile plasma, as described earlier.) Finally, we note that with ion heating a substantial number of fast neutrals can be generated, particularly in HANBIT, which has no hard wall-conditioning system such as the baking, and this will help further the edge density build-up through the increased wall recycling.

In summary, a larger density build-up is expected well in the $\omega < \omega_{ci}$ regime where the slow wave excitation and ion heating are possible. This additional density build-up will then greatly enhance the possibility of the $m = 1$ fast wave excitation by the slot antenna, providing a plausible explanation of why in HANBIT the stable high-density plasma mode with a radially peaked density profile is obtained in the $\omega < \omega_{ci}$ regime, rather than the $\omega > \omega_{ci}$ regime, unlike the other mirror devices.

4. Conclusion and future work

Initial physics experiments in the HANBIT mirror machine have shown the discharge characteristics to be quite different from those in other mirror machines. To explain the difference a model has been developed in which the absence of stable high-density modes in the $\omega > \omega_{ci}$ regime is attributed to the difficulty of the $m = 1$ fast wave excitation from the HANBIT slot antenna. Meanwhile, the high-density mode can be generated much more easily in the $\omega < \omega_{ci}$ regime because there both slow wave excitation and ion heating are possible, which can then greatly enhance the possibility of $m = 1$ fast wave excitation. While the model presented here can explain many features observed in the initial HANBIT experiments, there still remain many points that need more clarification. There is also a possibility that the observed mode transition may be related to the RF side-band coupling effect [7], which is known to give destabilization in the $\omega > \omega_{ci}$ regime, while stabilization in the $\omega < \omega_{ci}$ regime. A more careful check thus seems to still be necessary for a final conclusion.

Acknowledgment

This work is supported by the Korea Ministry of Science and Technology.

References

[1] Post R.S. *et al* 1987 *Proc. 11th Int. Conf. on Plasma Physics and Controlled Nuclear Fusion Research 1986 (Kyoto, 1986)* vol II (Vienna: IAEA) p 251

[2] Kwon M. *et al* 2001 *Trans. Fusion Technol.* **39** 10

[3] Golovato S.N. *et al* 1988 *Phys. Fluids* **31** 3744

[4] Yatsu K. *et al Potential Formation and Confinement in High Density Plasma on the GAMMA 10 Tandem Mirror* these proceedings (EX/P2-09)

[5] Kruglyakov E.P. *et al Axisymmetric Magnetic Mirrors for Plasma Confinement: Recent Progress and Perspectives* these proceedings (EX/C1-4Rb)

[6] Ferron J.R. *et al* 1983 *Phys. Rev. Lett.* **51** 1955

[7] McBride J.B. *et al* 1985 *Phys. Rev. Lett.* **54** 42

[8] Majeski R. *et al* 1987 *Phys. Rev. Lett.* **59** 206

[9] Yasaka Y. and Itatani R. 1983 *Phys. Rev. Lett.* **56** 2811

[10] Ko W.H. *et al* 2002 *Japan. J. Appl. Phys.* **41** 6209

[11] Pastukhov V.P. 1974 *Nucl. Fusion* **14** 3

[12] Yoon N.S. *et al* 1999 *Fusion Technol.* **35** 427

[13] Ferron J.R., Golovato S.N., Hershkowitz N. and Goulding R. 1987 *Phys. Fluids* **30** 1869